1521-0111/89/5/593–605$25.00
MOLECULAR PHARMACOLOGY

http://dx.doi.org/10.1124/mol.115.101832
Mol Pharmacol 89:593–605, May 2016

Fevipiprant (QAW039), a Slowly Dissociating CRTh2 Antagonist with the Potential for Improved Clinical Efficacy[S]

David A. Sykes, Michelle E. Bradley, Darren M. Riddy, Elizabeth Willard, John Reilly, Asadh Miah, Carsten Bauer, Simon J. Watson, David A. Sandham, Gerald Dubois, and Steven J. Charlton

Novartis Institutes for Biomedical Research, Horsham, West Sussex, UK (D.A.S., M.E.B., D.M.R., E.W., J.R., A.M., S.W., D.A.S., G.D., S.J.C.); Novartis Institutes for Biomedical Research, Cambridge, Massachusetts (D.A.Sa., J.R.); Novartis Institutes for Biomedical Research, Basel, Switzerland (C.B.); School of Life Sciences, Queen's Medical Centre, University of Nottingham, Nottingham, UK (D.A.Sy., S.J.C.)

Received September 22, 2015; accepted February 22, 2016

ABSTRACT

Here we describe the pharmacologic properties of a series of clinically relevant chemoattractant receptor-homologous molecules expressed on T-helper type 2 (CRTh2) receptor antagonists, including fevipiprant (NVP-QAW039 or QAW039), which is currently in development for the treatment of allergic diseases. [^{3}H]-QAW039 displayed high affinity for the human CRTh2 receptor (1.14 ± 0.44 nM) expressed in Chinese hamster ovary cells, the binding being reversible and competitive with the native agonist prostaglandin D_2 (PGD_2). The binding kinetics of QAW039 determined directly using [^{3}H]-QAW039 revealed mean kinetic on (k_{on}) and off (k_{off}) values for QAW039 of 4.5×10^7 $M^{-1}min^{-1}$ and 0.048 $minute^{-1}$, respectively. Importantly, the k_{off} of QAW039 (half-life = 14.4 minutes) was >7-fold slower than the slowest reference compound tested, AZD-1981. In functional studies, QAW039 behaved as an insurmountable antagonist of PGD_2-stimulated [^{35}S]-GTPγS activation, and its effects were not fully reversed by increasing concentrations of PGD_2 after an initial 15-minute incubation period. This behavior is consistent with its relatively slow dissociation from the human CRTh2 receptor. In contrast for the other ligands tested this time-dependent effect on maximal stimulation was fully reversed by the 15-minute time point, whereas QAW039's effects persisted for >180 minutes. All CRTh2 antagonists tested inhibited PGD_2-stimulated human eosinophil shape change, but importantly QAW039 retained its potency in the whole-blood shape-change assay relative to the isolated shape change assay, potentially reflective of its relatively slower off rate from the CRTh2 receptor. QAW039 was also a potent inhibitor of PGD_2-induced cytokine release in human Th2 cells. Slow CRTh2 antagonist dissociation could provide increased receptor coverage in the face of pathologic PGD_2 concentrations, which may be clinically relevant.

Introduction

The chemoattractant receptor-homologous molecule expressed on T-helper type 2 cells (CRTh2) is a class A G protein–coupled receptor involved in the modulation of inflammatory responses. CRTh2 (or DP_2) is also expressed on innate immune cells such as eosinophils, basophils (Nagata et al., 1999a,b), and group 2 lymphoid cells (ILC2) (Xue et al., 2014) and is known to play a role in the pathophysiology of airway disease.

Activation of CRTh2 receptors occurs via the natural ligand prostaglandin D_2 (PGD_2), a major product of the cyclooxygenase pathway released primarily by allergen activated mast cells (Miadonna et al., 1990) in asthmatic and allergic rhinitis patients. High levels of PGD_2 (Murray et al., 1986; Wenzel et al., 1989; Crea et al., 1992) lead to recruitment and activation of Th2 cells and stimulate eosinophil shape change and migration (Pettipher et al., 2007). PGD_2 also promotes increased CD11b expression, which facilitates cell adhesion on the vascular cell wall and movement of eosinophils from the circulation to the site of inflammation (Monneret et al., 2001; Gyles et al., 2006). Interestingly, severe asthmatics have been reported to accumulate a particular subtype of PGD_2-producing mast cells in the airway submucosa and epithelium resulting in increased sputum levels of PGD_2 relative to other steroid treated asthma patients (Balzar et al., 2011).

Stimulation of CRTh2 receptors found in the bronchial epithelium has been shown to drive epithelial differentiation, suggesting that, in addition to its well-characterized role in inflammatory cell migration, CRTh2 may contribute to airway remodeling in asthmatic patients (Stinson et al., 2015). Preclinical studies suggest that CRTh2 antagonism may also

dx.doi.org/10.1124/mol.115.101832.
[S] This article has supplemental material available at molpharm.aspetjournals.org.

ABBREVIATIONS: CHO, Chinese hamster ovary; CRTh2, chemoattractant receptor-homologous molecule expressed on T-helper type 2; DMSO, dimethylsulfoxide; DR, dose ratio; EC_{50}, molar concentration of an agonist that produces 50% of its maximal possible effect; E_{max}, maximal agonist effect; E_{min}, effect in absense of any agonist response; HSA, human serum albumin; IL, interleukin; K_d, equilibrium binding constant; k_{ob}, kinetic observed rate of association; k_{off}, kinetic off rate; k_{on}, kinetic on rate; MOA, mechanism of action; PGD_2, prostaglandin D_2; QAW039, 2-(2-methyl-1-1(4-(methylsulphonyl)-2-(trifluromethyl)benzyl)-1H-pyrrolo[2,3-b]pyridine-3-yl)acetic acid (fevipiprant); TP, thromboxane A_2 receptor; $t_{½}$, half-life.

potentially accelerate apoptosis and clearance of Th2 cells from inflamed tissue, thereby promoting the resolution of the underlying inflammation in allergic asthma and other related conditions such as allergic rhinitis (Xue et al., 2009). In animal models of acute allergen challenge PGD_2-mediated effects are blocked by CRTh2 antagonists acting on CRTh2 receptors on Th2 cells and inflammatory effector cells downstream of the allergic cascade (Uller et al., 2007). Several selective orally available antagonists have been since described in the literature, with compounds such as setipiprant (Diamant et al., 2014), BI-671800 (Krug et al., 2014), and OC-459 (Barnes et al., 2012) providing clinical proof of concept in asthma and allergic rhinitis. A comprehensive review of the current status of these and other compounds, including the dual CRTh2/thromboxane A_2 receptor (TP) antagonist ramatroban (Sugimoto et al., 2003), is available (Norman 2014).

Drug-receptor interactions are traditionally characterized in terms of potency and efficacy in preclinical screening programs; however, increasing evidence suggests that the time molecules reside at their cellular target can provide an important indicator of their clinical performance (Swinney, 2009). In functional assays, these slowly dissociating compounds exhibit the well documented phenomenon of "hemiequilibrium" (Charlton and Vauquelin, 2010), characterized functionally as a depressed agonist response and one that potentially can aid the selection of molecules for further preclinical development. For these reasons, we used the [^{35}S]-GTPγS assay format to assess the ability of CRTh2 antagonists to inhibit PGD_2 responses over time.

We recently reported the discovery of QAV680, a potent selective CRTh2 receptor antagonist, suitable for clinical testing in allergic diseases (Sandham et al., 2013). QAV680 dosed twice or four times daily was shown to reduce nasal symptom scores after allergen challenge in patients with allergic rhinitis (Erpenbeck et al., 2014a,b). A follow-up compound was consequently sought with improved duration of action (DOA) giving the potential for once-daily dosing to increase patient compliance. This optimization resulted in the discovery of 2-(2-methyl-1-1(4-(methylsulphonyl)-2-(trifluromethyl)benzyl)-1H-pyrrolo[2,3-b]pyridine-3-yl)acetic acid (QAW039, fevipiprant), which is currently in clinical development for asthma and atopic dermatitis.

Previous work has demonstrated different modes of action (MoA) of antagonists of CRTh2 receptors, for example, studies have suggested a noncompetitive MoA for the small-molecule antagonist AZD-1981 (Schmidt et al., 2013), whereas structurally similar compounds such as OC-459 and ramatroban have been shown to be competitive (Pettipher et al., 2012; Uller et al., 2007; Mathiesen et al., 2006). A complicating factor or explanation could be the phenomenon of hemiequilibrium resulting from slow dissociation, which leads to insurmountable antagonism under certain conditions and can be inadvertently mistaken for noncompetitive inhibition. The aim of the present study was to determine the binding characteristics of QAW039 and a cohort of clinically relevant reference antagonists at the human CRTh2 receptor and to explore the influence of kinetics on compound MoA by investigating the effect of these ligands on PGD_2-stimulated CRTh2 responses in both recombinant and relevant inflammatory cell types.

Materials and Methods

Cell Culture and Membrane Preparation

Chinese hamster ovary (CHO) cells expressing the human CRTh2 receptor were grown to 80%–90% confluence in 500 cm^2 cell culture plates at 37°C in 5% CO_2. All subsequent steps were conducted at 4°C to avoid receptor degradation. The cell culture media were removed, and ice-cold HBS-EDTA (1 × 10 ml; 10 mM HEPES, 0.9% w/v NaCl, 0.2% w/v EDTA pH 7.4) was added to the cells, which were then scraped from the plates into a 50-ml Corning tube and subsequently centrifuged at 250*g* for 5 minutes to allow a pellet to form. The supernatant fraction was aspirated, and 10 ml/500 cm^2 tray of wash buffer (10 mM HEPES, 10 mM EDTA, pH 7.4) was added to the pellet, which was homogenized using an electrical homogenizer "ultra-turrax" (position 6, 4 × 5-second bursts) and subsequently centrifuged at 48,000*g* at 4°C (Beckman Avanti J-251 Ultracentrifuge) for 30 minutes. The supernatant was discarded and the pellet rehomogenized and centrifuged, as described, in wash buffer. The final pellet was suspended in ice-cold 10 mM HEPES, 0.1 mM EDTA, pH 7.4, at a concentration of 5–10 mg ml^{-1}. Protein concentration was determined by the Bio-Rad Protein Assay based on the method of Bradford (1976), using bovine serum albumin as a standard. Membrane aliquots were maintained at −80°C until required.

Compounds

QAW039 was prepared using procedures reported for QAV680 (Sandham et al., 2013), and all reference CRTh2 antagonists were prepared according to patent procedures referenced in Lamers et al., (2013). The preparation of [^{3}H]-QAW039 has been previously described (see Luu et al., 2015). [^{3}H]-OC-459 was prepared by direct hydrogen isotope exchange on solid support. Further details, plus the structures, specific activity, and chemical purity of both radioligands, are provided in the Supplemental Materials.

Common Procedures Applying to [^{3}H]-QAW039 and [^{3}H]-OC-459 Radioligand Binding Experiments

All radioligand experiments were conducted in 96 deep-well plates in assay binding buffer (Hanks' balanced salt solution containing 10 mM HEPES, 1% dimethylsufoxide (DMSO), and 0.02% pluronic acid, pH 7.4) at 37°C. In all cases, nonspecific binding was determined in the presence of 3 μM AZD-1981, a selective CRTh2 antagonist. After the indicated incubation period, bound and free radioligand were separated by rapid vacuum filtration using a FilterMate Cell Harvester (PerkinElmer, Beaconsfield, UK) onto 96-well GF/B filter plates pretreated with assay buffer and rapidly washed three times with ice-cold wash buffer (20 mM HEPES containing 1 mM $MgCl_2$ pH 7.4). After drying (>4 hours), 40 μl of Microscint 20 (PerkinElmer) was added to each well and radioactivity quantified using single photon counting on a TopCount microplate scintillation counter (PerkinElmer). Aliquots of [^{3}H]-QAW039 and [^{3}H]-OC-459 were also quantified accurately to determine how much radioactivity was added to each well using liquid scintillation spectrometry on a Hidex 300SL scintillation counter (LabLogic, Sheffield, UK). In all experiments, total binding never exceeded more than 10% of that added, therefore limiting significant depletion of the free radioligand concentration (Carter et al., 2007). To ensure the experiment was at the described temperature, all components were prewarmed for ≥2 hours.

[^{3}H]-QAW039 and [^{3}H]-OC-459 Saturation Binding

Binding was performed with a range of concentrations of [^{3}H]-QAW039 and [^{3}H]-OC-459 to construct saturation binding curves, as described by Sykes et al., (2010). CHO-CRTh2 cell membranes (0.5 μg $well^{-1}$ respectively) were incubated in 96-deep well plates at 37°C in assay-binding buffer with gentle agitation for 3 hours to ensure equilibrium was reached. Owing to the low concentrations of [^{3}H]-QAW039 used,

the assay volume was increased to 1.5 ml to avoid significant depletion of the radioligand and unlabeled competitors.

[^{3}H]-QAW039 Competition Binding

To obtain affinity estimates for unlabeled QAW039 and the other unlabeled CRTh2 reference compounds, [^{3}H]-QAW039 displacement experiments were performed in a total reaction volume of 0.5 ml. [^{3}H]-QAW039 was used at a concentration of approximately 1 nM such that the calculated total binding never exceeded more than 10% of that added and therefore avoided ligand depletion. [^{3}H]-QAW039 was incubated in the presence of the indicated concentration of unlabeled CRTh2 antagonist and CHO cell membranes expressing the CRTh2 receptor (0.5 μg well^{-1} respectively) at 37°C in assay binding buffer containing GTPγS (30μM) in 96-deep well plates with gentle agitation for 2.5 hours to ensure equilibrium was reached. In a separate study designed to assess the MoA of QAW039, increasing concentrations of [^{3}H]-QAW039 (0.5, 1, 3, 10, 30$\times$ K_d) were incubated against increasing concentrations of unlabeled QAW039 (homologous binding) and increasing concentrations of the native agonist PGD_2 plus selected CRTh2 antagonists all in the presence of GTPγS (30 μM).

Determination of the Binding Kinetics of [^{3}H]-QAW039 at Human CRTh2 Receptors

To accurately determine the kinetic on (k_{on}) and off (k_{off}) rates, the observed rate of association (k_{ob}) was calculated with at least three different concentrations of [^{3}H]-QAW039 (0.3, 1, and 3$\times$ K_i). The appropriate concentration of [^{3}H]-QAW039 was incubated with CRTh2 CHO-cell membranes (0.5 μg well^{-1}) in assay binding buffer with gentle agitation (final assay volume 500 μl). The binding of [^{3}H]-QAW039 to the CRTh2 receptor was initiated with the addition of CHO cell membranes, and bound and free [^{3}H]-QAW039 were separated at the indicated time points to construct association kinetic curves. Care was taken to ensure that equilibrium was reached for each concentration before the experiment was terminated. After incubation, bound was separated from free by rapid filtration, plates were left to dry, and radioactivity was quantified (all as previously described).

Determination of the Dissociation Rate (k_{off}) of [^{3}H]-QAW039 and [^{3}H]-OC-459 at the Human CRTh2 Receptor

A single concentration of [^{3}H]-QAW039 (2.5 nM) and [^{3}H]-OC-459 (5 nM) was allowed to fully associate with human CRTh2 CHO cell membranes (0.5 μg well^{-1}) in a final reaction volume of 500 μl. To construct dissociation kinetic curves, an excess of AZD1981 (3 μM) was added at various time intervals to the reaction mixture to initiate dissociation of the radioligands. Dissociation was monitored for up to 150 minutes until [^{3}H]-QAW039 was fully dissociated from the human CRTh2 receptor. Bound and free [^{3}H]-QAW039 and [^{3}H]-OC-459 were separated at the indicated time points by rapid filtration, plates were left to dry, and radioactivity was quantified (all as previously described).

Competition Kinetics at Human CRTh2 receptors

The kinetic parameters of unlabeled QAW039 and the other CRTh2 antagonists were assessed using the methodology of Sykes et al., (2010). An experimentally calculated concentration of [^{3}H]-QAW039 (~2.5 nM, a concentration that avoided ligand depletion in this assay volume) was incubated with the indicated concentration(s) of unlabeled competitor in a final volume of assay binding buffer of 500 μl. Each time point was conducted on the same 96-deep-well plates incubated with constant gentle agitation. The experiment was initiated by the addition of CRTh2 CHO cell membranes (0.5 μg well^{-1}) containing GTPγS (30 μM), and the plates were harvested (as previously described) at the indicated time points.

[^{35}S]-GTPγS Functional Binding Assay

A range of concentrations of test compound were prepared in 100% DMSO, and 2.5 μl was added to a 96-well white OptiPlate. To each well, 200 μl of assay buffer (20 mM HEPES, 10 mM $MgCl_2$, 100 mM NaCl, and 1 mM EDTA) containing 0.1% human serum albumin (HSA), 30 μg ml^{-1} saponin (added fresh on the day of experimentation), 50 μg ml^{-1} CHO-CRTh2 membranes, 3.7 μM guanosine 5′-diphosphate sodium salt (GDP), 2.5 mg ml^{-1} WGA PVT SPA beads, and 50 μl of [^{35}S]-guanosine 5′-(γ-thio)triphosphate ([^{35}S]-GTPγS) at a concentration of 300 pM was added and incubated at room temperature with gentle agitation for 2 hours. After this incubation, 2.5 μl of increasing concentrations of PGD_2 prepared at 100$\times$ concentration in 100% DMSO was added and incubated at room temperature with gentle agitation for 15, 60, 120, and 180 minutes. Eleven concentrations of PGD_2 were studied in total. After this, the plates were centrifuged for 3 minutes at 1000g and bound [^{35}S]-GTPγS quantified using single-photon counting on a TopCount microplate scintillation counter (PerkinElmer).

Isolated Eosinophil Shape-Change Assay

Granulocytes were isolated from the blood of healthy normal volunteers. The granulocytes were incubated with PGD_2 for 5 minutes at 37°C. The reaction was terminated by addition of CellFixTM, and data were acquired on FACSCalibur flow cytometer, first with FSC/SSC plots and then FSC/FL-2 to distinguish eosinophils from neutrophils. Data were fitted to a sigmoidal curve (Origin 7 or XL fit) to give a typical EC_{50} for PGD_2 of 0.72 ± 0.11 nM (n = 3, data not shown). Antagonist curves were determined as follows: aliquots of granulocyte in assay buffer containing 1% dimethylsulfoxide (DMSO) were treated with aliquots of 10 increasing test compound concentrations, and the mixture was incubated for 5 minutes at 37°C. Agonist (EC_{70} concentration) was added, and the mixture was incubated for a further 5 minutes. The reaction was terminated and activity measured as already described. Data were fitted to a sigmoidal curve (Origin 7 or XL Fit) to give an IC_{50} value.

Whole-Blood Eosinophil Shape-Change Assay

Blood was collected into sterile 3.8% (w/v) trisodium citrate from healthy atopic volunteers and used immediately with minimum disturbance. Agonist curves were determined as follows: aliquots of whole blood (80 μl) were incubated in assay buffer containing 1% DMSO for 5 minutes at 37°C. Increasing concentrations of PGD_2 were added, and the mixture was incubated with gentle shaking at 37°C for 5 minutes. The reaction was terminated by the addition of ice-cold CellFixTM (250 μl), followed by ammonium chloride lysis solution (1.5 ml). After incubation on ice for 40–60 minutes, data were acquired on FACSCalibur flow cytometer, first with FSC/SSC plots and then FSC/FL-2 to distinguish eosinophils from neutrophils. Data were fitted to a sigmoidal curve (Origin 7 or XL fit) to give a typical EC_{50} for PGD_2 of 0.94 ± 0.18 nM (n = 3, data not shown). Antagonist curves were determined as follows: aliquots of whole blood (80 μl) and test compound (10 concentrations) were incubated in assay buffer containing 1% DMSO for 5 minute at 37°C. Agonist (EC_{70} concentration in 10 μl in assay buffer) was added, and the mixture was incubated with gentle shaking at 37°C for 5 minutes. The reaction was terminated and samples measured as described herein.

Th2 Cell Cytokine-Release Assay

CRTh2$^+$ Th2 cells isolated by either MACS or MoFlo (see Supplemental Materials) were counted and seeded in flat-bottom 96-well plates at a concentration of 100,000 cells/well. Cells were seeded in X-VIVO 15 medium plus 10% human AB serum and 1% penicillin/streptomycin. QAW039 was applied to the cells at a range of concentrations between 1000 and 0.3 nM and incubated with the cells (37°C, 5% CO_2) for 30 minutes. PGD_2 then was added to the cells at a final concentration of 200 nM. Unstimulated cells were included in the

assay and cells treated with medium alone; PGD_2 at 200 nM ± vehicle (0.01% DMSO) was also included as a control. Once all additions had been made, the plate was incubated for a further 6 hours at 37°C, 5% CO_2, after which the plate was centrifuged at 400*g* for 10 minutes, and the supernatant was harvested into 96-well plates and stored at -20°C before cytokine analysis was carried out. The supernatant samples were analyzed for levels of the Th2 cytokines interleukin (IL)-13, IL-5, and IL-4 and also IL-12 (as a negative control) using the Mesoscale Discovery human IL-13 issue culture assay kit plus detection antibodies for human IL-4, IL-5, and IL-12 (total). Briefly, 25 μl of each Calibrator (standard) at a range of 10,000–2.4 pg/ml was applied to the plate in duplicate and 25 μl of neat test sample in triplicate. The plate was then incubated at room temperature for 2 hours with shaking at 800 rpm. Then 25 μl of the detection antibody solution mix (each antibody diluted 1 in 50 in antibody dilution buffer) was added to each well and incubated for a further 2 hours at room temperature with shaking at 800 rpm. The plate was then washed three times in phosphate-buffered saline containing 0.05% Tween-20 and 150 μl of 2× Read buffer T was added to each well. The plate was analyzed on the SECTOR Imager, and the results for each cytokine were analyzed using Discovery Workbench software. IC_{50} values were calculated using GraphPad Prism v4.0 software.

Interpretation of Data

Data Analysis. As the amount of radioactivity varied slightly for each experiment (<5%), data are shown graphically as the mean ± S.D. for individual representative experiments, whereas all values reported in the text and tables are mean ± S.E.M. for the indicated number of experiments. All experiments were analyzed by nonlinear regression using Prism 6.0 (GraphPad Software, San Diego, U.S.A.). Competition displacement binding data were fitted to sigmoidal (variable slope) curves using a four-parameter logistic equation (eq. 1):

$$Y = \text{Bottom} + (\text{Top} - \text{Bottom}) / \left(1 + 10^{(\log EC_{50} - X).\text{Hillcoefficient}}\right) \quad (1)$$

IC_{50} values obtained from the inhibition curves were converted to K_i values using the method of Cheng and Prusoff (1973). [^{3}H]-QAW039 association data were fitted as follows to a global fitting model using GraphPad Prism 6.0 to simultaneously calculate k_{on} and k_{off} using the eq. 2, where k_{ob} equals the observed rate of association:

$$k_{ob} = [\text{Radioligand}] \cdot k_{on} + k_{off} \quad (2)$$

Association and dissociation rates for unlabeled antagonists were calculated using eq. 3–10 described by Motulsky and Mahan (1984):

$$K_A = k_1[L] + k_2 \quad (3)$$

$$K_B = k_3[I] + k_4 \quad (4)$$

$$S = \sqrt{\left((K_A - K_B)^{\,2 + 4 \cdot k_1 \cdot k_3 \cdot L \cdot I \cdot 10^{-18}}\right)} \quad (5)$$

$$K_F = 0.5 \cdot (K_A + K_B + S) \quad (6)$$

$$K_S = 0.5 \cdot (K_A + K_B - S) \quad (7)$$

$$DIFF = K_F - K_S \quad (8)$$

$$Q = \frac{B_{max} \cdot K_1 \cdot L \cdot 10^{-9}}{DIFF} \quad (9)$$

$$Y = Q \cdot \left(\frac{k4 \cdot DIFF}{K_F \cdot K_S} + \frac{k_4 - K_F}{K_F} \cdot \exp^{(-K_F \cdot X)} - \frac{k_4 - K_s}{K_s} \cdot \exp^{(-K_S \cdot X)}\right) \quad (10)$$

where X is the time (min), Y is the specific binding (cpm), $k_1 = k_{on}$ [^{3}H]-QAW039, $k_2 = k_{off}$ [^{3}H]-QAW039, L is the concentration of [^{3}H]-QAW039 used (nM), B_{max} is the total binding (cpm), and I is the concentration unlabeled antagonist (nM).

Fixing the preceding parameters allowed the following to be calculated: k_3 = association rate of unlabeled ligand (M^{-1} min^{-1}), k_4 = dissociation rate of unlabeled ligand (min^{-1}).

Dissociation of [^{3}H]-QAW039 and [^{3}H]-OC-459 was fitted to a one-phase monoexponential decay function to estimate the dissociation rate of QAW039 and OC-459 directly.

PGD_2 stimulated [^{35}S]-GTPγS binding data were fitted as sigmoidal (variable slope) curves using the four-parameter logistic equation, and the negative logarithm to base 10 of the molar concentration of an antagonist that makes it necessary to double the concentration of the agonist required to elicit the original submaximal response obtained in the absence of antagonist (pA2). pA2 values were estimated directly from Schild analysis after normalization of data to the control maximal response (see Supplemental Fig. 3 and Supplemental Table 1). Specifically, data were fitted using a four-parameter logistic equation in Prism 6.0 as described already [each curve was fit to its own value of n, the molar concentration of an agonist that produces 50% of its maximal possible effect (EC_{50}), effect in the absence of any agonist response (E_{min}) and maximal agonist effect (E_{max})] and to a simpler model (where a common E_{min}, E_{max}, and n values were used). When the F statistic indicated that a significantly better fit was obtained with the simple model, dose ratios (DRs) were calculated for construction of Schild plots. Data were then fitted to the Gaddum-Schild equation in Prism 6.0 to obtain an estimation of the Schild slope. If the Schild slope did not differ significantly from unity (F test), the data were refit to a slope of 1.0 to derive pA2 values. Corrected pA2 estimates were derived by correcting for % bound to HSA (0.1%) using the method of Toutain and Bousquet-Melou (2002). The validity of this correction is borne out of the fact that plasma-protein binding (Table 3) and HSA binding are directly correlated for the CRTh2 antagonists tested in this study ($P < 0.0001$, $r^2 = 0.97$ data not shown). For a full explanation of this conversion and the effects of protein on apparent receptor affinity, see Blakeley et al. (2015). PGD_2 did not reach equilibrium with QAW039 in the time frame of the GTPγS assay, so EC_{30} estimates were taken, from which we were able to estimate log DR-1 values to derive a Schild plot and obtain a pA2 value. Estimated pA2 values along with corrected estimated pA2 estimates are shown in Supplemental Table 1.

Functional GTPγS data for QAW039 were fitted according to a combined operational and hemiequilibrium model for competitive antagonism under nonequilibrium conditions (Kenakin, 2009; Mould et al., 2014; Riddy et al., 2015) to derive kinetic parameters for QAW039 as in eq. 11–14:

$$\alpha = \frac{[B]/K_B}{([B]/K_B + [A]/K_A + 1)} \quad (11)$$

$$\beta = \frac{[B]/K_B}{([B]/K_B + 1)} \quad (12)$$

$$\gamma = \frac{([B]/K_B + [A]/K_A + 1)}{([A]/K_A + 1)} \quad (13)$$

$$Y = \frac{[A]/K_A(1 - (\alpha \cdot (1 - e^{-koff \cdot \gamma \cdot t}) + \beta \cdot e^{-koff \cdot \gamma \cdot t})) \cdot \tau \cdot E_m}{[A]/K_A((1 - (\alpha \cdot (1 - e^{-koff \cdot \gamma \cdot t}) + \beta \cdot e^{-koff \cdot \gamma \cdot t})) \cdot \tau + 1) + 1}, \quad (14)$$

where [A] and [B] represent the concentrations of PGD_2 and QAW039, respectively; K_A and K_B represent the respective equilibrium dissociation constants; k_{off} is the dissociation rate constant for the antagonist (min^{-1}); t is the assay incubation time (min); τ is the operational efficacy of PGD_2; and E_m is the maximal system response. All parameters were shared across all data sets except t, which were fixed to the assay incubation time. In all cases, potency and affinity values were estimated as logarithms (Christopoulos, 1998). Data shown are the mean ± S.E.M. (see Supplemental Fig. 4).

Results

QAW039 and Related CRTh2 Compounds. The structure of QAW039 and related CRTh2 antagonists and the agonist indomethacin are shown in Fig. 1. QAW039 is a

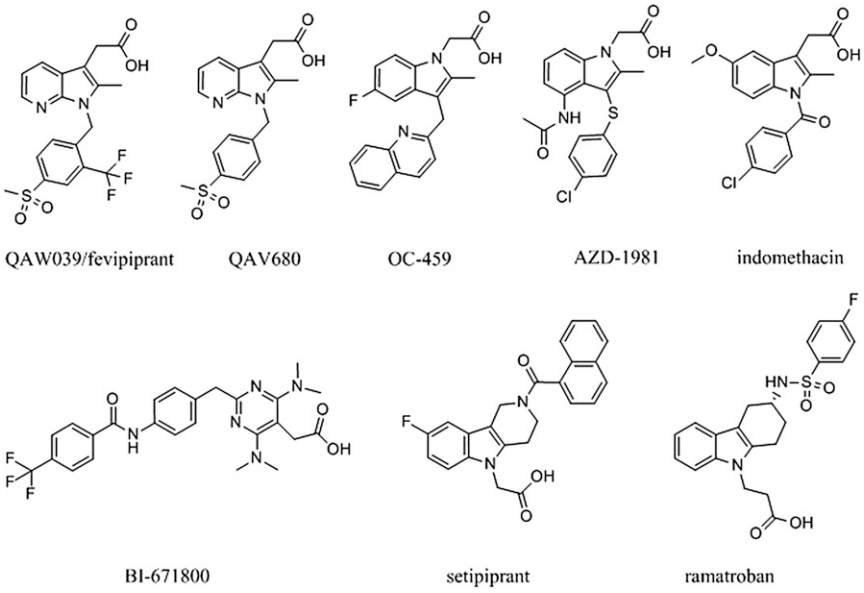

Fig. 1. Structures of the selective CRTh2 antagonist QAW039 and reference CRTh2 ligands.

triuoromethyl derivative of the previously described 7-azaindole-3-acetic acid QAV680 (Sandham et al., 2013). The measured lipophilicity ($logD_{7.4}$) of these compounds is lower than other described CRTh2 antagonists (Table 3), which likely contributes to their lower plasma-protein binding.

Characterization of CHO-CRTh2-Expressing Cell Line. Specific [^{3}H]-QAW039 and [^{3}H]-OC-459 binding to human CRTh2 receptors in CHO membranes was saturable and best described by the interaction of the radioligand with a single population of high-affinity sites. A representative saturation binding curve for [^{3}H]-QAW039 and [^{3}H]-OC-459 binding to the human CHO-CRTh2 receptor is shown in Fig. 2, A and B. The expression level of the CHO-CRTh2 in the CHO cell line and the corresponding equilibrium dissociation constant (K_d) of [^{3}H]-QAW039 and [^{3}H]-OC-459 determined from saturation binding studies are shown in Table 1.

Determination of the Dissociation Rate (k_{off}) of [^{3}H]-QAW039 and [^{3}H]-OC-459 at the Human CRTh2 Receptor. A single concentration of [^{3}H]-QAW039 (2.5 nM) and [^{3}H]-OC-459 (5 nM) was allowed to fully associate with the human CRTh2 receptor. An excess of AZD-1981 (3 μM) was then added to the reaction mixture to initiate dissociation of [^{3}H]-QAW039 and [^{3}H]-OC-459. Dissociation was monitored until [^{3}H]-QAW039, and [^{3}H]-OC-459 was fully dissociated

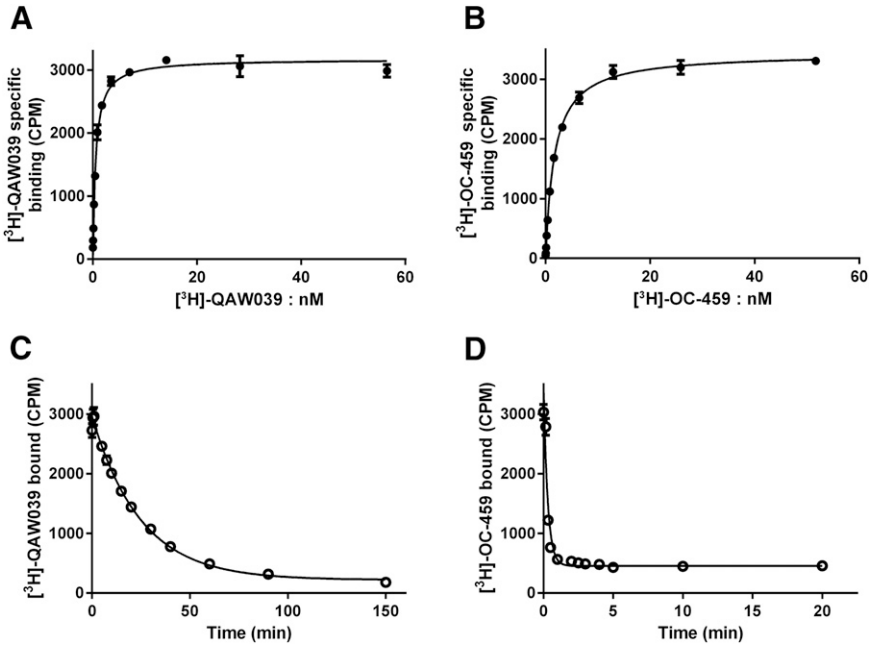

Fig. 2. Characterization of the CRTh2 radioligands [^{3}H]-QAW039 and [^{3}H]-OC-459. Saturation binding of [^{3}H]-QAW039 (A) and [^{3}H]-OC-459 (B) to human CRTh2 receptors expressed in membranes from CHO cells. Dissociation of [^{3}H]-QAW039 (C) and [^{3}H]-OC-459 (D) from human CRTh2 receptors expressed in membranes from CHO cells. Data are shown as mean ± S.E.M. and are representative of three separate experiments performed in triplicate.

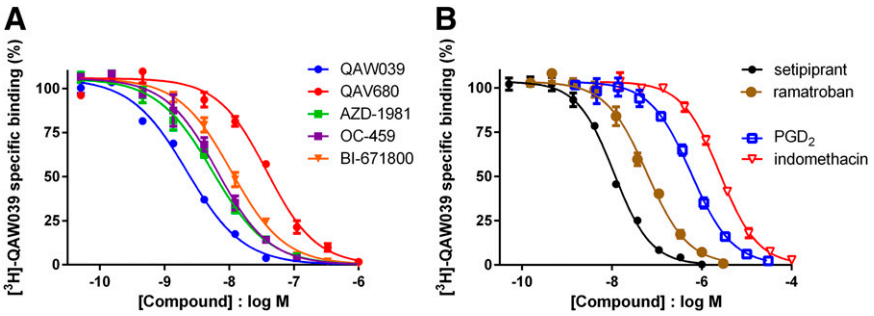

Fig. 3. Competition binding between [^{3}H]-QAW039 and CRTh2 receptor ligands for human CRTh2 receptors expressed in membranes from CHO cells. Displacement of [^{3}H]-QAW039 (1 nM) by increasing concentrations of CRTh2 antagonist (A) QAW039, QAV680, AZD-1981, OC-459, and BI-671800 and (B) setipiprant and ramatroban plus the CRTh2 agonists PGD_2 and indomethacin. Data are presented as the mean range from a representative of three experiments performed in duplicate.

from the human CRTh2 receptor (Fig. 1, C and D). The data were fitted to a monoexponential decay function to estimate a k_{off} value for QAW039 and OC-459 directly. A k_{off} value of 0.050 ± 0.006 minute^{-1} [half-life ($t_{1/2}$) = 14.2 minutes] was determined for the slowly dissociating [^{3}H]-QAW039 and a value of 2.80 ± 0.53 minute^{-1} ($t_{1/2}$ = 0.28 minutes) for the more rapidly dissociating [^{3}H]-OC-459 binding to human CRTh2 receptors.

Determination of the Equilibrium Binding Affinity Constant of CRTh2 Antagonists and Agonists at CRTh2 Receptors. IC_{50} values determined from competition binding experiments were converted to equilibrium binding constants (pK_i) by using the equation of Cheng and Prusoff (1973) and using the K_d value of [^{3}H]-QAW039 as described in *Materials and Methods*. The competition binding curves showing displacement of [^{3}H]-QAW039 by QAW039 and the other CRTh2 compounds tested are shown in Fig. 3, A and B, and the affinity values (pK_i) for CRTh2 antagonist and agonist binding to human CRTh2 receptors are summarized in Table 2.

Determination of the Kinetic Parameters of [^{3}H]-QAW039 at the Human CRTh2 Receptor. To calculate the kinetic on (k_{on}) and off rates (k_{off}) of the unlabeled QAW039 and the other CRTh2 antagonists, the kinetic parameters of the radioligand, [^{3}H]-QAW039 were first determined. A family of association kinetic curves was constructed using a range of [^{3}H]-QAW039 concentrations. Each association curve was monitored until equilibrium so that Y_{max} was reached (Fig. 4A). From this type of analysis, it is possible to estimate both k_{on} and k_{off} values for QAW039 by fitting the data to a global kinetic model. A k_{on} value for [^{3}H]-QAW039 of 4.52 ± 0.45 × 10^7 M^{-1} min^{-1} and a k_{off} value of 0.048 ± 0.005 min^{-1} was determined. From the k_{off} value, a $t_{1/2}$ of dissociation (0.693/k_{off}) of 14.4 minutes was calculated for [^{3}H]-QAW039. K_{ob} increased in a linear manner with [^{3}H]-QAW039 concentration (Fig. 4B), and the mean kinetic parameters estimated from these plots were in good agreement, with values estimated from the global fit described herein (linear fit mean k_{off} = 0.044 ± 0.004 min^{-1} and k_{on} = 4.86 ± 0.53 × 10^7 M^{-1} min^{-1}).

Determination of the Kinetic Parameters of QAW039 and Competitor Compounds at Human CRTh2 Receptors. Using the equations described in *Materials and Methods* and the kinetic values obtained for [^{3}H]-QAW039, as detailed already, the association and dissociation rates for unlabeled QAW039, OC-459, and the other CRTh2 antagonists for the human CRTh2 (Figs. 4, C and D; Table 2; and Supplemental Fig. 1, A–E, respectively) receptor were calculated. The kinetic on (k_{on}) and off rates (k_{off}) determined for QAW039 using the Motulsky-Mahan method were not significantly different from the values calculated from the global kinetic analysis, suggesting that [^{3}H]-QAW039 is suitable for the determination of kinetic parameters of unlabeled CRTh2 antagonists. To validate the rate constants, the kinetically derived dissociation constant (K_d) values (k_{off}/k_{on}) were compared with the dissociation constant (K_i) obtained from equilibrium competition binding experiments. Good correlation (r^2 = 0.95, $P < 0.001$, data not shown) was found between these two values, indicating that the kinetic parameters were accurate.

QAW039 is a Competitive Antagonist of the Native CRTh2 Receptor Agonist PGD_2. To explore the nature of the interaction of QAW039 with the CRTh2 receptor we used the technique of competitive binding. Using this technique, we have explored the inhibitory potency of unlabeled QAW039, AZD-1981, OC-459, and the native agonist PGD_2 over a range of concentrations of [^{3}H]-QAW039 designed to saturate the receptor. At the lowest radioligand concentration used, ~0.3 nM, the pIC_{50} value for displacement by QAW039 itself was 9.05 ± 0.10 (Fig. 5A). As expected, a linear increase in the pIC_{50} value was obtained as the radioligand concentration was increased to the maximum concentration used in the study, ~30 nM (~30-fold greater than K_d from saturation binding) (Fig. 5E). This same pattern of behavior was mimicked by the other

TABLE 1

Saturation binding and dissociation kinetic rate constant (k_{off}) data for [^{3}H]-QAW039 and [^{3}H]-OC-459 binding to human CRTh2 receptors

Data are mean ± S.E.M. from at least three separate experiments.

Radioligand	Receptor Expression Level	Dissociation Kinetic Rate Constant k_{off}	Equilibrium Dissociation Constant K_d
	pmol mg^{-1}	*min^{-1}*	*nM*
[^{3}H]-QAW039	6.26 ± 0.51	0.050 ± 0.006	1.14 ± 0.44
[^{3}H]-OC-459	6.44 ± 0.06	2.80 ± 0.53	2.44 ± 0.58

TABLE 2
Kinetic and equilibrium binding parameters of unlabeled QAW039 and other CRTh2 ligands interacting with the human CRTh2 receptor
Data are mean ± S.E.M. from at least three separate experiments.

CRTh2 Ligand	k_{on}	k_{off}	$t_{1/2}$	Kinetic pK_d	Equilibrium pK_i
	$M^{-1}min^{-1}$	min^{-1}	min		
QAW039	$6.27 \pm 0.93 \times 10^7$	0.061 ± 0.006	12.04	8.99 ± 0.06	8.98 ± 0.03
QAV680	$4.80 \pm 2.14 \times 10^7$	0.66 ± 0.18	1.29	7.82 ± 0.04	7.54 ± 0.09
AZD-1981	$3.01 \pm 0.76 \times 10^8$	0.77 ± 0.23	1.26	7.58 ± 0.02	8.49 ± 0.03
OC-459	$9.50 \pm 5.14 \times 10^8$	1.83 ± 0.32	0.41	8.61 ± 0.17	8.35 ± 0.13
BI-671800	$2.47 \pm 0.36 \times 10^8$	1.22 ± 0.11	0.58	8.30 ± 0.01	8.14 ± 0.20
Ramatroban	$1.89 \pm 0.66 \times 10^7$	0.80 ± 0.22	1.10	7.33 ± 0.05	7.45 ± 0.02
Setipiprant	$1.87 \pm 0.45 \times 10^8$	0.95 ± 0.15	0.76	8.28 ± 0.04	8.35 ± 0.06
PGD_2	nd	nd	nd	nd	6.41 ± 0.08
Indomethacin	nd	nd	nd	nd	5.74 ± 0.12

nd, Not determined.

structurally related CRTh2 antagonists and PGD_2 which were investigated in parallel. The difference in pIC_{50} values for unlabeled PGD_2 were precisely in line with those predicted by the Cheng-Prusoff relationship (Cheng and Prusoff, 1973), using the K_d value for QAW039 obtained from saturation binding (Table 1), suggesting that unlabeled PGD_2 displaced the radioligand competitively.

Determination of the Effect CRTh2 Antagonists on PGD_2 Stimulated [^{35}S]-GTPγS Binding to Human CRTh2 Receptors. To investigate the potential for QAW039 and the other CRTh2 antagonists to display insurmountable behavior in a [^{35}S]-GTPγS binding assay, PGD_2 concentration response curves were constructed in the presence of increasing concentrations of pre-equilibrated antagonist (Fig. 6). [^{35}S]-GTPγS binding to CHO-hCRTh2 membranes was measured at different time intervals after incubation with the endogenous CRTh2 agonist PGD_2. QAW039 produced a clear reduction in the E_{max} of PGD_2 stimulated GTPγS binding after a 15-minute incubation period, with PGD_2 (Fig. 6A) demonstrating its ability to produce insurmountable antagonism in a functionally relevant second-messenger reporter assay. The incubation was extended to 180 minutes to allow the PGD_2 to reach equilibrium with the receptor and fully activate a second-messenger response. The inhibitory effect of QAW039 was readily reversible with time; however, the inhibitory effects of QAW039 were not fully reversed even after a 180-minute incubation period with PGD_2 (see Supplemental Fig. 2 and Supplemental

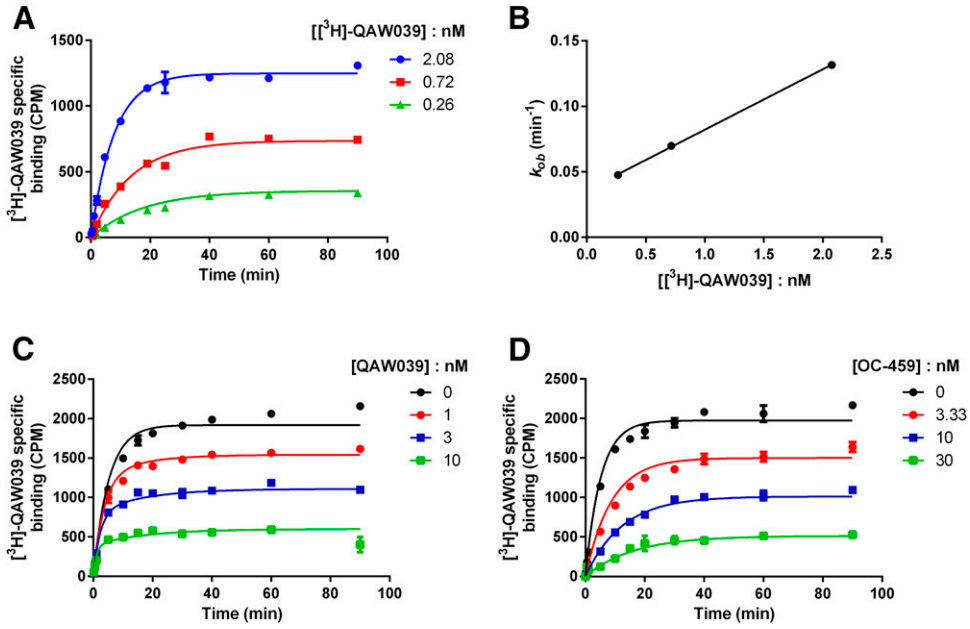

Fig. 4. Direct determination of [^{3}H]-QAW039 kinetic binding parameters plus competition kinetic binding to determine the kinetic rate constants of unlabeled compounds. (A) Association of [^{3}H]-QAW039 to the human CRTh2 receptor expressed in membranes from CHO cells. A family of association kinetic curves was constructed using a range of [^{3}H]-QAW039 concentrations. The k_{on} and k_{off} values for QAW039 were determined by fitting the data to a global kinetic association model. (B) Plot of ligand concentration verses k_{ob}. Binding followed a simple law of mass action model, k_{ob} increasing in a linear manner with radioligand concentration. [^{3}H]-QAW039 competition kinetic curves in the presence of unlabeled QAW039 (C) and OC-459 (D). CHO-CRTh2 membranes were incubated with ~2.5 nM [^{3}H]-QAW039 and increasing concentrations of unlabeled competitor. Plates were incubated at 37°C for the indicated time points and nonspecific binding levels were determined in the presence of 3 μM AZD-1981. Data were fitted to the equations described in *Materials and Methods* to calculate k_{on} and k_{off} values for the unlabeled ligands; these are summarized in Table 2. Data are presented as mean ± range from representative three or more experiments performed in duplicate.

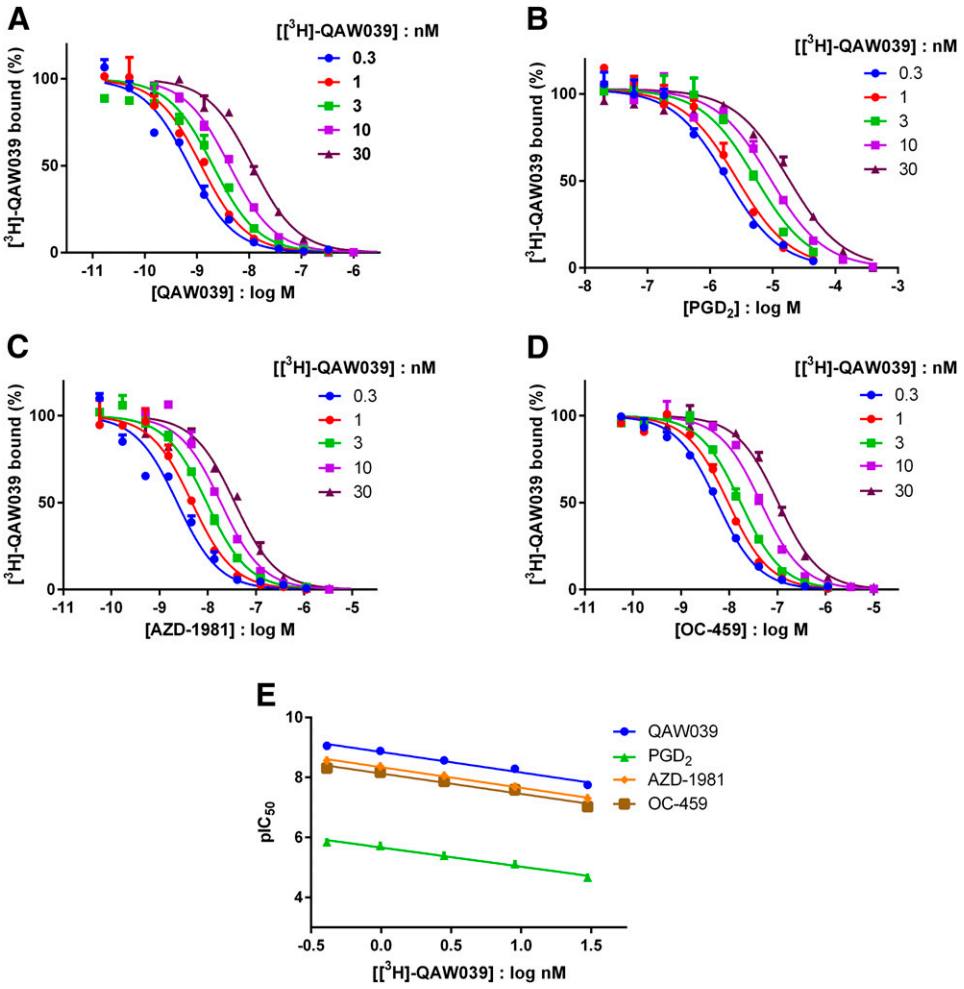

Fig. 5. Determination of the competitive mode of action of QAW039 with PGD_2 and the selected other CRTh2 antagonists. Effect of increasing concentrations of [^{3}H]-QAW039 on the degree of inhibition observed with increasing concentrations of (A) QAW039, (B) PGD_2, (C) AZD-1981, and (D) OC-459 at human CRTh2 receptors expressed in membranes from CHO cells. (E) Linear increase in the compound pIC_{50} values with increasing [^{3}H]-QAW039 concentrations. Data are shown as mean ± range and are representative of three separate experiments performed in duplicate.

Fig. 3). Also apparent was a reduction in the basal accumulation of GTPγS binding in the presence of increasing concentrations of QAW039 and the other CRTh2 antagonists (Fig. 6). This finding demonstrates that these compounds behave as inverse agonists of CRTh2 mediated GTPγS accumulation. In contrast to QAW039, the more rapidly dissociating CRTh2 antagonists tested did not produce any noticeable depression of the PGD_2 maximal response after 15 minutes of incubation (Fig. 6, B–G). PGD_2-stimulated [^{35}S]-GTPγS binding in the presence of these more rapidly dissociating CRTh2 compounds after a 180-minute incubation period is shown for comparison with QAW039 (see Supplemental Fig. 2 and 3, B–G, respectively).

It is not possible to accurately derive pK_B values directly from the GTPγS binding experiments since the compounds are bound to plasma proteins (e.g., HSA; Table 3), resulting in irregular shifts of the PGD_2 concentration response curves at concentrations of compound that come close to saturating the protein (0.1% HSA or 15 μM) present in the assay buffer. Once HSA gradually becomes saturated by the increasing concentrations of antagonist, the Schild slopes become gradually steeper as more antagonist becomes free in solution and available to bind the CRTh2 receptor (i.e., deviation from constant % bound; see Blakeley et al., 2015). As would be predicted, this effect is most pronounced for the low CRTh2 affinity, highly protein-bound compound setipiprant (see Supplemental Fig. 3G); however, Schild plots of the lower concentrations of QAW039, QAV680, AZD-1981, OC-459, BI-671800, and ramatroban (<10 μM, i.e., below the saturating protein concentration) tested resulted in Schild slopes not significantly different from 1.0 and pA2 values and in line with expected pK_i estimates after correction for HSA binding, further suggesting that these compounds are behaving competitively with PGD_2 (see Table 2, Supplemental Fig. 3, and Supplemental Table 1). Although PGD_2 did not fully reach equilibrium with QAW039 in the 180-minute time frame of the GTPγS assay, we previously determined it to be competitive with PGD_2 based on competitive binding data; hence, we have estimated DR-1 values to derive a Schild plot and obtain an estimated pA2 value. Thus, the [^{35}S]-GTPγS competition assay data are entirely consistent with the radioligand competition binding analysis and suggest that these molecules interact with the same orthosteric binding pocket as PGD_2.

When a comparison of CRTh2 antagonist inhibitory potency was made at the 15-minute time point in the [^{35}S]-GTPγS assay, after the addition of a maximally effective concentration of PGD_2 (1μM), the superior potency of QAW039 compared with the other CRTh2 compounds tested in this study was clearly visible (Fig. 7). This result suggests that the kinetic off rate potentially could play a role in driving the superior potency of this compound.

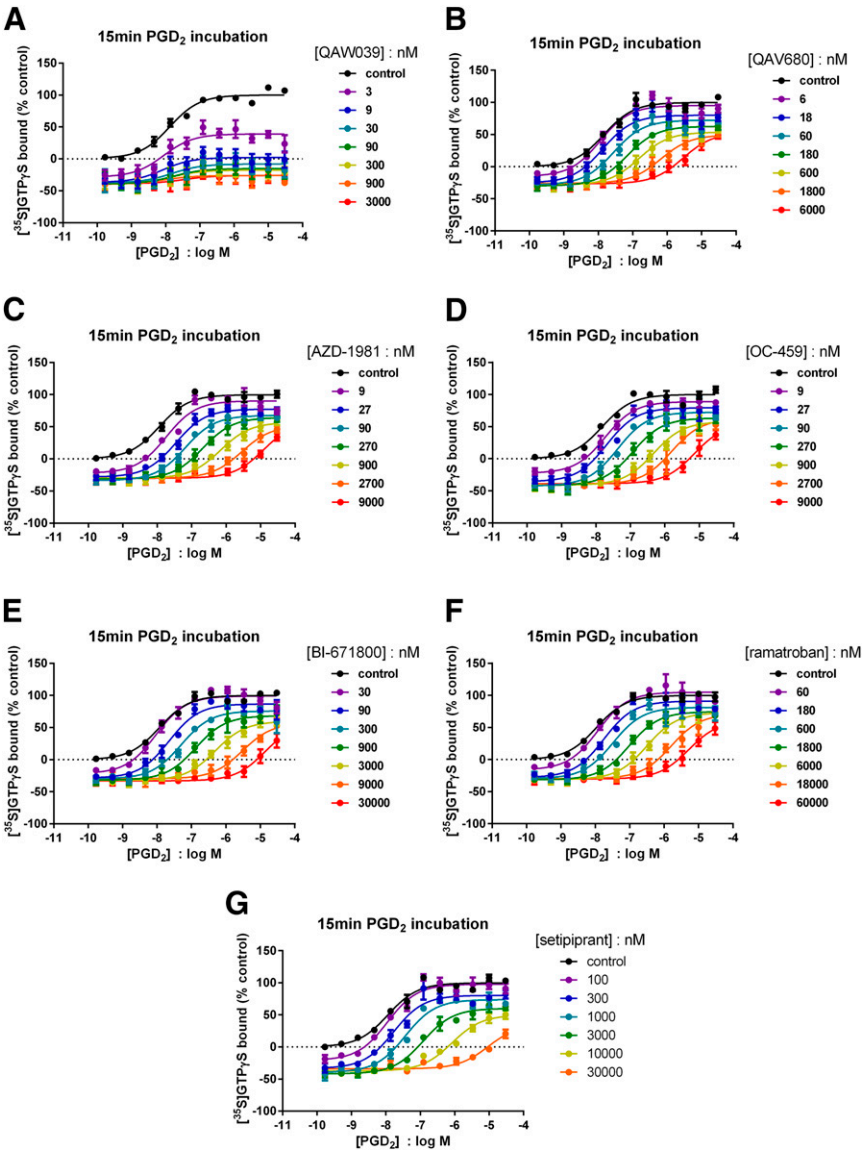

Fig. 6. Effect of CRTh2 antagonists on PGD_2-stimulated GTPγS accumulation. Insurmountable behavior of (A) QAW039 at human CRTh2 receptors expressed in membranes from CHO cells after a 15-minute incubation period with the agonist PGD_2. Surmountable behavior of (B) QAV680, (C) AZD-1981, (D) OC-459, (E) BI-671800, (F) ramatroban, and (G) setipiprant after a 15-minute incubation period. Data are shown as mean ± S.E.M. and are representative of three separate experiments performed in singlet.

The effect of time on the potency of CRTh2 antagonists to inhibit PGD_2 (1μM)-stimulated GTPγS accumulation is shown in Fig. 8. QAW039 is >10-fold more effective at inhibiting the PGD_2 response after a 15-minute incubation compared with the full 180-minute incubation period (Fig. 8A), reflecting its very slow dissociation from the CRTh2 receptor in the face of high concentrations of PGD_2. The other CRTh2 antagonist examined are equieffective at all time points,

TABLE 3

CRTh2 antagonist human whole-blood (WBSC) and isolated cellular (ISC) shape-change potency values plus protein binding and physicochemical descriptors clogP, $logD_{7.4}$, and $logK_{IAM}$

Data are mean ± S.E.M. for three or more experiments.

CRTh2 Antagonist	cLogP	Log $D_{7.4}$a	log $K_{IAM7.4}$b	% Human Plasma Protein Unboundc	WBSC IC_{50}	ISC IC_{50}
					nM	*nM*
QAW039	2.26	0.65	1.12	7.8	0.44 ± 0.19	0.40 ± 0.04
QAV680	1.15	−0.34	0.55	21.4	31.0 ± 1.0	5.0 ± 1.0
AZD-1981	4.79	1.19	1.77	1.8	13.10 ± 4.03	2.21 ± 0.87
OC-459	4.57	1.32	1.91	0.5	422.5 ± 155.9	6.4 ± 1.4
BI-671800	4.58	1.65	1.95	0.4	104.9 ± 35.3	1.87 ± 0.88
Ramatroban	3.97	1.34	1.89	2.7	195 ± 75.4	11.4 ± 1.9
Setipiprant	4.28	1.35	1.88	0.4	>500	10.7 ± 1.7

[a]Determined by high-performance liquid chromatography (HPLC) column method (Kerns et al., 2003).
[b]Determined by HPLC column method (Valko et al., 2000).
[c]Determined by equilibrium dialysis (Banker et al., 2003).

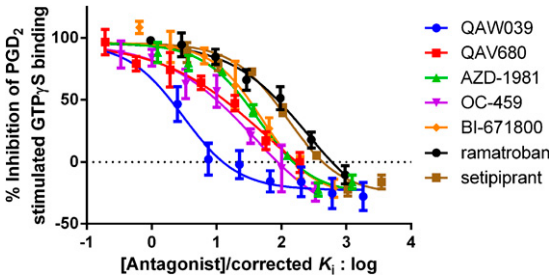

Fig. 7. Functional consequences of hemiequilibrium. Effect of CRTh2 antagonists acting at human CRTh2 receptors expressed in membranes from CHO cells on % depression of a maximally effective concentration of PGD_2 (1μM) in the [^{35}S]-GTPγS assay at the 15-minute time point. Antagonist potency is expressed as a ratio of concentration added over compound affinity corrected for % HSA bound. Data are shown as mean ± S.E.M. from three separate experiments performed in singlet.

demonstrating that kinetics does not play any role in determining their potency under these experimental conditions (Fig. 8, B–G).

An estimate of the affinity and dissociation rate of the CRTh2 antagonist QAW039 from functional [^{35}S]-GTPγS data after a 60-minute incubation was obtained by fitting data according to an operational hemiequilibrium model for competitive antagonism first described by Kenakin (2009) and recently used practically to estimate the dissociation rates of orexin-2 antagonists and muscarinic M_1 antagonists in functional assays (Mould et al., 2014; Riddy et al., 2015) (see Supplemental Fig. 4 and Supplemental Table 2). A pA_2 value for QAW039 of 3.2 ± 0.7 nM was estimated, which is very much in line with affinity estimates obtained from kinetic association experiments performed at room temperature (K_d 1.39 ± 0.23 nM; see Supplemental Fig. 5 and Supplemental Table 3) and the pA2 obtained from the Schild analysis (see Supplemental Table 1). Importantly, the k_{off} value for QAW039 of 0.005min^{-1} was also within 3-fold of that estimated in kinetic association binding experiments performed at room temperature (QAW039 k_{off} = 0.012 ± 0.001 min^{-1}; see Supplemental Fig. 5 and Supplemental Table 3), demonstrating the potential for the GTPγS assay to identify very slowly dissociating compounds. In contrast, it was not possible to fit other ligands to the operational hemiequilibrium model as their effects were fully reversible within the 15-minute incubation period. Confirmation that [^{3}H]-OC-459 was relatively rapidly dissociating when profiled at room temperature comes from kinetic association binding experiments (see Supplemental Fig. 5 and Supplemental Table 3).

Determination of the Effect of QAW039 on PGD_2 Stimulated Whole-Blood Eosinophil Shape-Change. Migration of eosinophils from the microcirculation into sites of inflammation occurs as a consequence of cytoskeletal rearrangements in a process known as eosinophil shape change. Purified human eosinophils undergo shape change on exposure to PGD_2 in response to activation of CRTh2 and a similar response is seen in whole blood. This study confirms the inhibitory effect of the tested CRTh2 antagonists in both the isolated and whole-blood shape-change assays. QAW039 was the most potent compound tested at inhibiting PGD_2 stimulated eosinophil shape change, with comparable potencies in both the isolated and whole blood shape-change assays (Table 3).

Determination of the Effect of QAW039 on Cytokine Release from PGD_2 Stimulated CD4+ Th2 Cells. The chronic inflammatory response characteristically observed in allergic asthma occurs by the selective accumulation of Th2 lymphocytes, which further potentiate the inflammatory response by releasing Th2 cytokines such as IL-5 and IL-13. The localized increase in the release of Th2 cytokines at the primary site of inflammation causes activation of Th2 cells, eosinophils, and basophils. Here we have shown that QAW039 is a potent inhibitor of PGD_2-induced release of IL-5 and IL-13 from human CD4$^+$ Th2 lymphocytes (Table 4). The potency of QAW039 in this cellular functional assay system is 15- to 20-fold greater than the previous lead compound QAV680.

Discussion

It is potentially advantageous when developing antagonists of G protein–coupled receptors to identify compounds that exhibit slow dissociation from the receptor (Tummino and Copeland 2008). CRTh2 antagonists exhibiting such behavior may display greater clinical efficacy as a consequence of prolonged receptor blockade, which will effectively reduce the recruitment of proinflammatory eosinophils into existing areas of inflammation. Such a profile could be particularly important in the asthmatic lung, where local concentrations of PGD_2 are likely to vary depending on the numbers of activated mast cells, especially given that PGD_2 release occurs in a matter of minutes after IgE activation (Kawata et al., 1995). Importantly, the transit time of mixed leukocytes across the pulmonary circulation has recently been quantified and is thought to be similar to that of neutrophils measured precisely at 14.2 seconds, only marginally slower than that reported for RBCs (Summers et al., 2014). This implies that sustained CRTh2 blockade will protect against eosinophil recruitment as they transit through areas of high PGD_2 concentration in the lung. Clinical data generated with QAW039 in eosinophilic asthmatics show a reduction in both sputum and tissue bronchial biopsy eosinophils, supporting this hypothesis (Berair et al., 2015). Prolonged CRTh2 receptor blockade therefore represents a new and potentially powerful approach for the treatment of allergic asthma.

The binding properties of several clinically relevant CRTh2 antagonists, including the recently developed QAW039, were determined at the human CRTh2 receptor in assay buffer containing physiologic sodium ion concentration at 37°C. Previous studies designed to assess the kinetics of unlabeled CRTh2 antagonists have used nonphysiologic assay conditions, experiments being conducted at room temperature in the absence of salt (Gervais et al., 2011). Findings from these early kinetic studies are therefore likely to overestimate the receptor target coverage since it has been well documented that compound kinetics is highly dependent on temperature and sodium ion concentration (Sykes et al., 2012). This phenomenon was also apparent in the current study, with the off rates of QAW039 and OC-459 being up to 5-fold slower when measured at room temperature compared with 37°C.

Other researchers have attempted to estimate dissociation $t_{1/2}$s indirectly from functional [^{35}S]-GTPγS assays performed at room temperature by measuring responses to PGD_2 (100 μM) at fixed time periods following a 60-minute preincubation period with test compounds, allowing antagonist $t_{1/2}$ values to

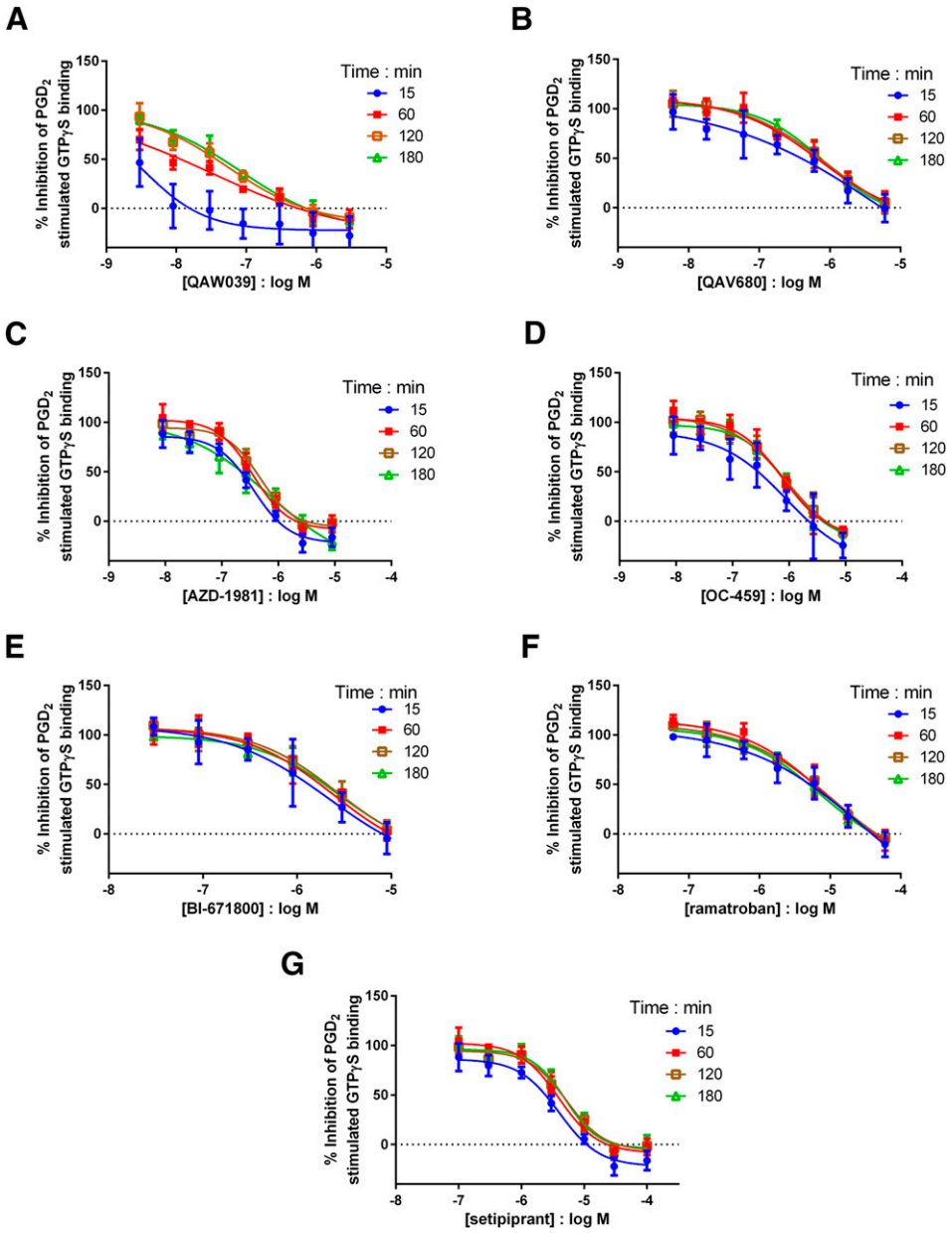

Fig. 8. Effects of hemiequilibrium on CRTh2 antagonist potency. The effect of time on the inhibitory potency of CRTh2 antagonists (A) QAW039, (B) QAV680, (C) AZD-1981, (D) OC-459, (E) BI-671800, (F) ramatroban, and (G) setipiprant in the [^{35}S]-GTPγS binding assay after stimulation of the CRTh2 receptor expressed in membranes from CHO cells with a maximal effective concentration of PGD_2 (1 μM). Data are shown as mean ± S.E.M. and of three separate experiments performed in singlet.

be estimated by fitting an exponential decay curve to the PGD_2 responses observed over time (Andrés et al., 2014). Although these results enabled a rank order of residence time to be established, the use of an accumulation assay mean the dissociation $t_{½}$ values are likely to be overestimated.

TABLE 4

Comparison of potencies of CRTh2 antagonists QAV680 and QAW039 for inhibition of PGD_2-induced cytokine release in human CD4+ Th2 lymphocytes

Data are mean ± S.E.M. from at least three separate experiments.

CRTh2 Antagonist	Inhibition of IL-5 Release IC_{50}	Inhibition of IL-13 Release IC_{50}
	nM	*nM*
QAW039	2.56 ± 1.24	1.40 ± 0.30
QAV680	57 ± 28	29 ± 5

In saturation binding experiments, [^{3}H]-QAW039 and [^{3}H]-OC-459 display nM affinity for the human CRTh2 receptor expressed in CHO cells. The mean kinetic k_{on} and k_{off} values determined for [^{3}H]-QAW039 were 4.5×10^7 $M^{-1}min^{-1}$ and 0.048 min^{-1}, respectively, producing a $t_{1/2}$ value of 12 minutes and a kinetic K_d value of 1.06 ± 0.06 nM, which is in excellent agreement with the equilibrium K_d value obtained in the saturation binding experiments described here. In contrast, despite displaying comparable nM affinity, OC-459 was ~30× faster at dissociating from the CRTh2 receptor ($t_{1/2}$ = 0.41 minute). To put this in context, >50% of OC-459 could potentially be displaced from the CRTh2 receptor in the time it takes for eosinophils to pass through the asthmatic lung, whereas in direct contrast, <1.2% of QAW039 will likely become displaced in the same time frame.

The binding kinetics of unlabeled QAW039 and the other related CRTh2 antagonists including OC-459 were also determined indirectly using [^{3}H]-QAW039 as the tracer through

application of a competition binding model first described by Motulsky and Mahan (1984). The kinetic K_d values generated indirectly were in agreement with the K_i values generated by equilibrium competition kinetic binding, validating use of the current methods. The pharmacologic properties of QAW039 are a significant improvement on those of our original lead compound, QAV680, and the other CRTh2 antagonists examined in this study. In particular, QAW039 is significantly slower to dissociate from the CRTh2 receptor (>9-fold compared with QAV680), which potentially affords this compound increased efficacy and an improved duration of action at the CRTh2 receptor due to sustained blockade of the receptor in the face of increasing concentrations of PGD_2. This phenomenon of insurmountability is highlighted in the GTPγS assay, where QAW039, which exhibits the slowest dissociation rate constant, also produced the most pronounced suppression of the maximal response to PGD_2 in the GTPγS binding assay. The slower the compound k_{off}, the greater the % inhibition achieved in the GTPγS binding assay for any given multiple of the compound K_i added. QAW039 displays a time-dependent inhibitory effect in the GTPγS binding assay, its potency being highest at early time points (Fig. 8A), characteristic of its slow dissociation from the CRTh2 receptor. This effect may contribute to QAW039's increased potency in the eosinophil whole-blood shape-change assay relative to the more rapidly dissociating reference compounds.

The detailed pharmacologic analysis presented in this study confirms the competitive nature of QAW039 and structurally related ligands binding to the human CRTh2 receptor. In particular, the observation that the pIC_{50} for PGD_2 displacement of [^{3}H]-QAW039 binding (to the CRTh2 receptor) increased in a linear fashion with equivalent pA2 values at increasing radioligand concentration demonstrates that QAW039 behaves as a simple competitive antagonist. Similarly, PGD_2 itself and the two other reference CRTh2 antagonists examined, OC-459 and AZD-1981, appeared fully competitive, with increasing concentrations of QAW039 demonstrating that all these molecules occupy the same CRTh2 receptor binding pocket.

Limited information exists on the MoA of other CRTh2 antagonists, but previous publications using functional assays have highlighted potential insurmountable antagonist profiles (Mathiesen et al., 2006; Gervais et al., 2011). Both publications attribute this compound profile to slow receptor dissociation kinetics whereby equilibrium between PGD_2 and receptor is not achieved in the time frame of their experiments. In contrast, AZD-1981 has been shown to exhibit a noncompetitive binding profile, despite possessing rapid dissociation kinetics (Schmidt et al., 2013), as demonstrated using an agonist ([^{3}H]-PGD_2) binding assay and could potentially result from stabilization of the uncoupled form of the CRTh2 receptor.

In functional studies performed at room temperature and in salt containing buffer, QAW039 behaves as an insurmountable antagonist of PGD_2-stimulated GTPγS activation after a 15-minute agonist equilibration time. This insurmountable behavior is entirely consistent with QAW039's relatively slow dissociation ($t_{1/2}$ = 14.4 minutes) from the human CRTh2 receptor, but it does not result from a noncompetitive interaction. Thus, the time-dependent concentration-dependent rightward shifts observed with QAW039 in the human GTPγS assay, coupled with the Schild analysis (Fig. 8A; and see Supplemental Fig. 3), support the findings of homologous binding studies (see Fig. 5) and demonstrate that QAW039 behaves as a simple competitive antagonist of PGD_2 functional responses.

To investigate the profile QAW039 at the cellular level, we chose two relevant inflammatory cell types. CRTh2-mediated shape change in eosinophils was used to profile QAW039 in whole blood and represents a physiologically relevant environment. The comparable IC_{50} values for QAW039 in the whole blood and isolated shape-change assays are consistent with its lower plasma-protein binding and its relatively slow dissociation kinetics that drive its increased potency (Fig. 8A). Other compounds showed large discrepancies between these two assay formats, which are likely the result of higher plasma-protein binding coupled with rapid dissociation from the CRTh2 receptor. In the case of QAV680, the reduced protein binding does not compensate for the faster dissociation kinetics. These data demonstrate that QAW039 is highly potent in whole-blood systems, with the IC_{50} value obtained consistent with the affinity values calculated from radioligand experiments. In a further disease-relevant cellular context, the potency of QAW039 in the isolated Th2 cell cytokine inhibition assay is consistent with its CRTh2 receptor affinity, and, as with eosinophil assay readouts, this represents an improved potency compared with QAV680.

In summary, in these human functional studies across diverse cellular systems, we have determined that the potency of QAW039 is cell type and cell function independent. Importantly, the pharmacologic profile determined for QAW039 suggests it should competitively inhibit other disease relevant CRTh2-mediated responses in human cells, including Th2 cell cytokine production, PGD_2-mediated Th2 cell apoptosis, basophil chemotaxis, and eosinophil activation. To our knowledge, this is the first study to demonstrate in both binding and functional studies the simple competitive antagonist nature of clinically relevant CRTh2 antagonists, including the slowly dissociating compound QAW039, and represents an important step forward in our understanding of the pharmacology of low-molecular-weight CRTh2 antagonists in competition with their native agonist PGD_2. QAW039 (fevipiprant) is under ongoing clinical study as a novel oral therapy for allergic diseases.

Authorship Contributions

Participated in research design: Sykes, Dubois, Charlton.

Conducted experiments: Sykes, Riddy, Bradley, Willard, Reilly, Miah.

Contributed new reagents or analytic tools: Bauer, Watson.

Performed data analysis: Sykes, Riddy, Bradley, Willard, Reilly, Miah.

Wrote or contributed to writing on manuscript: Sykes, Sandham, Charlton.

References

Andrés M, Buil MA, Calbet M, Casado O, Castro J, Eastwood PR, Eichhorn P, Ferrer M, Forns P, and Moreno I et al. (2014) Structure-activity relationships (SAR) and structure-kinetic relationships (SKR) of pyrrolopiperidinone acetic acids as CRTh2 antagonists. *Bioorg Med Chem Lett* **24**:5111–5117.

Balzar S, Fajt ML, Comhair SA, Erzurum SC, Bleecker E, Busse WW, Castro M, Gaston B, Israel E, and Schwartz LB et al. (2011) Mast cell phenotype, location, and activation in severe asthma. Data from the Severe Asthma Research Program. *Am J Respir Crit Care Med* **183**:299–309.

Banker MJ, Clark TH, and Williams JA (2003) Development and validation of a 96-well equilibrium dialysis apparatus for measuring plasma protein binding. *J Pharm Sci* **92**:967–974.

Barnes N, Pavord I, Chuchalin A, Bell J, Hunter M, Lewis T, Parker D, Payton M, Collins LP, and Pettipher R et al. (2012) A randomized, double-blind, placebo-controlled

study of the CRTH2 antagonist OC000459 in moderate persistent asthma. *Clin Exp Allergy* **42**:38–48.
Berair R, Gonem S, Singapuri A, Hartley R, Laurencin M, Bacher G, Holzhauer B, Bourne M, Mistry V, Pavord I, Mansur AH, Wardlaw A, Siddiqui S, Kay R, and Brightling CE. Effect of QAW039, an oral prostaglandin D_2 receptor (DP_2/CRTh2) antagonist, upon sputum and bronchial eosinophilic inflammation and clinical outcomes in treatment-resistant asthma: a phase 2a randomized placebo-controlled trial. *Am. J. Respir. Crit. Care. Med.*, **2015**, 191, A636.
Blakeley D, Sykes DA, Ensor P, Bertran E, Aston PJ, and Charlton SJ (2015) Simulating the influence of plasma protein on measured receptor affinity in biochemical assays reveals the utility of Schild analysis for estimating compound affinity for plasma proteins. *Br J Pharmacol* **172**:5037–5049.
Bradford MM (1976) A rapid and sensitive method for the quantitation of microgram quantities of protein utilizing the principle of protein-dye binding. *Anal Biochem* **72**:248–254.
Carter CM, Leighton-Davies JR, and Charlton SJ (2007) Miniaturized receptor binding assays: complications arising from ligand depletion. *J Biomol Screen* **12**: 255–266.
Charlton SJ and Vauquelin G (2010) Elusive equilibrium: the challenge of interpreting receptor pharmacology using calcium assays. *Br J Pharmacol* **161**: 1250–1265.
Cheng Y and Prusoff WH (1973) Relationship between the inhibition constant (K1) and the concentration of inhibitor which causes 50 per cent inhibition (I50) of an enzymatic reaction. *Biochem Pharmacol* **22**:3099–3108.
Christopoulos A (1998) Assessing the distribution of parameters in models of ligand-receptor interaction: to log or not to log. *Trends Pharmacol Sci* **19**:351–357.
Crea AE, Nakhosteen JA, and Lee TH (1992) Mediator concentrations in bronchoalveolar lavage fluid of patients with mild asymptomatic bronchial asthma. *Eur Respir J* **5**:190–195.
Diamant Z, Sidharta PN, Singh D, O'Connor BJ, Zuiker R, Leaker BR, Silkey M, and Dingemanse J (2014) Setipiprant, a selective CRTH2 antagonist, reduces allergen-induced airway responses in allergic asthmatics. *Clin Exp Allergy* **44**:1044–1052.
Erpenbeck VJ, Salapatek AM, Patel P, Sanni J, Dubois G, Zhou P, Perry S, and Larbig M. Efficacy and safety of 10 day treatment with the CRTh2 antagonist QAV680 evaluated in patients with allergic rhinitis in an environmental exposure chamber. *Eur. Resp. J.* **2014**, *44*, suppl 58 (poster P4075).
Erpenbeck VJ, Salapatek AM, Patel P, Carew D, Dubois G, Perry S, and Larbig M QAV680, cetirizine and their combination reduce nasal symptoms in patients with intermittent allergic rhinitis in an Environmental Exposure Chamber. *Eur. Resp. J.* **2014**, *44*, suppl 58 (poster P4069).
Gervais FG, Sawyer N, Stocco R, Hamel M, Krawczyk C, Sillaots S, Denis D, Wong E, Wang Z, and Gallant M et al. (2011) Pharmacological characterization of MK-7246, a potent and selective CRTH2 (chemoattractant receptor-homologous molecule expressed on T-helper type 2 cells) antagonist. *Mol Pharmacol* **79**:69–76.
Gyles SL, Xue L, Townsend ER, Wettey F, and Pettipher R (2006) A dominant role for chemoattractant receptor-homologous molecule expressed on T helper type 2 (Th2) cells (CRTH2) in mediating chemotaxis of CRTH2+ CD4+ Th2 lymphocytes in response to mast cell supernatants. *Immunology* **119**:362–368.
Kawata R, Reddy ST, Wolner B, and Herschman HR (1995) Prostaglandin synthase 1 and prostaglandin synthase 2 both participate in activation-induced prostaglandin D_2 production in mast cells. *J Immunol* **155**:818–825.
Kerns EH, Di L, Petusky S, Kleintop T, Huryn D, McConnell O, and Carter G (2003) Pharmaceutical profiling method for lipophilicity and integrity using liquid chromatography-mass spectrometry. *J Chromatogr B Analyt Technol Biomed Life Sci* **791**:381–388.
Kenakin TP (2009) Orthosteric drug antagonism, in *A Pharmacology*, 3rd ed. (Kenakin T, ed) pp 105–127, Elsevier Academic Press, London.
Krug N, Gupta A, Badorrek P, Koenen R, Mueller M, Pivovarova A, Hilbert J, Wetzel K, Hohlfeld JM, and Wood C (2014) Efficacy of the oral chemoattractant receptor homologous molecule on TH2 cells antagonist BI 671800 in patients with seasonal allergic rhinitis. *J Allergy Clin Immunol* **133**:414–419.
Lamers C, Flesch D, Schubert-Zsilavecz M, and Merk D (2013) Novel prostaglandin receptor modulators: a patent review (2002 - 2012) - part I: non-EP receptor modulators. *Expert Opin Ther Pat* **23**:47–77.
Luu VT, Goujon JY, Meisterhans C, Frommherz M, and Bauer C (2015) Synthesis of a high specific activity methyl sulfone tritium isotopologue of fevipiprant (NVP-QAW039). *J Labelled Comp Radiopharm* **58**:188–195.
Mathiesen JM, Christopoulos A, Ulven T, Royer JF, Campillo M, Heinemann A, Pardo L, and Kostenis E (2006) On the mechanism of interaction of potent surmountable and insurmountable antagonists with the prostaglandin D2 receptor CRTH2. *Mol Pharmacol* **69**:1441–1453.
Miadonna A, Tedeschi A, Brasca C, Folco G, Sala A, and Murphy RC (1990) Mediator release after endobronchial antigen challenge in patients with respiratory allergy. *J Allergy Clin Immunol* **85**:906–913.
Monneret G, Gravel S, Diamond M, Rokach J, and Powell WS (2001) Prostaglandin D2 is a potent chemoattractant for human eosinophils that acts via a novel DP receptor. *Blood* **98**:1942–1948.
Motulsky HJ and Mahan LC (1984) The kinetics of competitive radioligand binding predicted by the law of mass action. *Mol Pharmacol* **25**:1–9.
Mould R, Brown J, Marshall FH, and Langmead CJ (2014) Binding kinetics differentiates functional antagonism of orexin-2 receptor ligands. *Br J Pharmacol* **171**:351–363.
Murray JJ, Tonnel AB, Brash AR, Roberts LJ, 2nd, Gosset P, Workman R, Capron A, and Oates JA (1986) Release of prostaglandin D2 into human airways during acute antigen challenge. *N Engl J Med* **315**:800–804.
Nagata K, Hirai H, Tanaka K, Ogawa K, Aso T, Sugamura K, Nakamura M, and Takano S (1999b) CRTH2, an orphan receptor of T-helper-2-cells, is expressed on basophils and eosinophils and responds to mast cell-derived factor(s). *FEBS Lett* **459**:195–199.
Nagata K, Tanaka K, Ogawa K, Kemmotsu K, Imai T, Yoshie O, Abe H, Tada K, Nakamura M, and Sugamura K et al. (1999a) Selective expression of a novel surface molecule by human Th2 cells in vivo. *J Immunol* **162**:1278–1286.
Norman P (2014) Update on the status of DP2 receptor antagonists; from proof of concept through clinical failures to promising new drugs. *Expert Opin Investig Drugs* **23**:55–66.
Pettipher R, Hansel TT, and Armer R (2007) Antagonism of the prostaglandin D2 receptors DP1 and CRTH2 as an approach to treat allergic diseases. *Nat Rev Drug Discov* **6**:313–325.
Pettipher R, Vinall SL, Xue L, Speight G, Townsend ER, Gazi L, Whelan CJ, Armer RE, Payton MA, and Hunter MG (2012) Pharmacologic profile of OC000459, a potent, selective, and orally active D prostanoid receptor 2 antagonist that inhibits mast cell-dependent activation of T helper 2 lymphocytes and eosinophils. *J Pharmacol Exp Therap* **340**:473–482.
Riddy DM, Valant C, Rueda P, Charman WN, Sexton PM, Summers RJ, Christopoulos A, and Langmead CJ (2015) Label-free kinetics: exploiting functional hemi-equilibrium to derive rate constants for muscarinic receptor antagonists. *Mol Pharmacol* **88**:779–790.
Sandham DA, Arnold N, Aschauer H, Bala K, Barker L, Brown L, Brown Z, Budd D, Cox B, and Docx C et al. (2013) Discovery and characterization of NVP-QAV680, a potent and selective CRTh2 receptor antagonist suitable for clinical testing in allergic diseases. *Bioorg Med Chem* **21**:6582–6591.
Schmidt JA, Bell FM, Akam E, Marshall C, Dainty IA, Heinemann A, Dougall IG, Bonnert RV, and Sargent CA (2013) Biochemical and pharmacological characterization of AZD1981, an orally available selective DP2 antagonist in clinical development for asthma. *Br J Pharmacol* **168**:1626–1638.
Stinson SE, Amrani Y, and Brightling CE (2015) D prostanoid receptor 2 (chemoattractant receptor-homologous molecule expressed on TH2 cells) protein expression in asthmatic patients and its effects on bronchial epithelial cells. *J Allergy Clin Immunol* **135**:395–406.
Sugimoto H, Shichijo M, Iino T, Manabe Y, Watanabe A, Shimazaki M, Gantner F, and Bacon KB (2003) An orally bioavailable small molecule antagonist of CRTH2, ramatroban (BAY u3405), inhibits prostaglandin D2-induced eosinophil migration in vitro. *J Pharmacol Exp Ther* **305**:347–352.
Summers C, Singh NR, White JF, Mackenzie IM, Johnston A, Solanki C, Balan KK, Peters AM, and Chilvers ER (2014) Pulmonary retention of primed neutrophils: a novel protective host response, which is impaired in the acute respiratory distress syndrome. *Thorax* **69**:623–629.
Sykes DA, Dowling MR, and Charlton SJ (2010) Measuring receptor target coverage: a radioligand competition binding protocol for assessing the association and dissociation rates of unlabeled compounds. *Curr Protoc Pharmacol*. Chapter 9: Unit 9.14.
Sykes DA, Dowling MR, Leighton-Davies J, Kent TC, Fawcett L, Renard E, Trifilieff A, and Charlton SJ (2012) The Influence of receptor kinetics on the onset and duration of action and the therapeutic index of NVA237 and tiotropium. *J Pharmacol Exp Ther* **343**:520–528.
Swinney DC (2009) The role of binding kinetics in therapeutically useful drug action. *Curr Opin Drug Discov Devel* **12**:31–39.
Toutain PL and Bousquet-Melou A (2002) Free drug fraction vs free drug concentration: a matter of frequent confusion. *J Vet Pharmacol Ther* **25**:460–463.
Tummino PJ and Copeland RA (2008) Residence time of receptor-ligand complexes and its effect on biological function. *Biochemistry* **47**:5481–5492.
Uller L, Mathiesen JM, Alenmyr L, Korsgren M, Ulven T, Högberg T, Andersson G, Persson CG, and Kostenis E (2007) Antagonism of the prostaglandin D2 receptor CRTH2 attenuates asthma pathology in mouse eosinophilic airway inflammation. *Respir Res* **8**:16.
Valko K, Du CM, Bevan CD, Reynolds DP, and Abraham MH (2000) Rapid-gradient HPLC method for measuring drug interactions with immobilized artificial membrane: comparison with other lipophilicity measures. *J Pharm Sci* **89**:1085–1096.
Wenzel SE, Westcott JY, Smith HR, and Larsen GL (1989) Spectrum of prostanoid release after bronchoalveolar allergen challenge in atopic asthmatics and in control groups. An alteration in the ratio of bronchoconstrictive to bronchoprotective mediators. *Am Rev Respir Dis* **139**:450–457.
Xue L, Barrow A, and Pettipher R (2009) Interaction between prostaglandin D and chemoattractant receptor-homologous molecule expressed on Th2 cells mediates cytokine production by Th2 lymphocytes in response to activated mast cells. *Clin Exp Immunol* **156**:126–133.
Xue L, Salimi M, Panse I, Mjösberg JM, McKenzie AN, Spits H, Klenerman P, and Ogg G (2014) Prostaglandin D2 activates group 2 innate lymphoid cells through chemoattractant receptor-homologous molecule expressed on TH2 cells. *J Allergy Clin Immunol* **133**:1184–1194.

Addresses correspondence to: Dr. David Sandham, Global Discovery Chemistry, Novartis Institutes of Biomedical Research, 100 Technology Square, Cambridge MA 02139. E-mail: david.sandham@novartis.com or Prof. Steven Charlton, School of Life Sciences, Queen's Medical Centre, University of Nottingham, University of Nottingham, UK. E-mail: StevenCharlton@nottingham.ac.uk